A Versatile Nanotrap for Biochemical and Functional Studies with Fluorescent Fusion Proteins*[S]

Ulrich Rothbauer‡, Kourosh Zolghadr‡, Serge Muyldermans§, Aloys Schepers¶, M. Cristina Cardoso‖, and Heinrich Leonhardt‡**

Green fluorescent proteins (GFPs) and variants thereof are widely used to study protein localization and dynamics. We engineered a specific binder for fluorescent proteins based on a 13-kDa GFP binding fragment derived from a llama single chain antibody. This GFP-binding protein (GBP) can easily be produced in bacteria and coupled to a monovalent matrix. The GBP allows a fast and efficient (one-step) isolation of GFP fusion proteins and their interacting factors for biochemical analyses including mass spectroscopy and enzyme activity measurements. Moreover GBP is also suitable for chromatin immunoprecipitations from cells expressing fluorescent DNA-binding proteins. Most importantly, GBP can be fused with cellular proteins to ectopically recruit GFP fusion proteins allowing targeted manipulation of cellular structures and processes in living cells. Because of the high affinity capture of GFP fusion proteins *in vitro* and *in vivo* and a size in the lower nanometer range we refer to the immobilized GFP-binding protein as GFP-nanotrap. This versatile GFP-nanotrap enables a unique combination of microscopic, biochemical, and functional analyses with one and the same protein. ***Molecular & Cellular Proteomics 7:282–289, 2008.***

After the identification of most components of the cell, further insights into their regulation and function require information on their abundance, localization, and dynamic interactions. Green fluorescent proteins (GFPs)[1] and spectral variants thereof became popular tools to determine protein localization and, in combination with fluorescence photobleaching techniques, provided unique information on protein dynamics in living cells (1–4). Necessary additional information on DNA binding, enzymatic activity, and complex formation can be obtained with various methods including chromatin immunoprecipitation (ChIP) and affinity purification (5, 6). These methods, however, are hampered by the limited availability of specific antibodies. Those limitations are often bypassed by fusing the protein of interest to specific epitope or protein tags including hemagglutinin, c-Myc, FLAG, or GST (7, 8). Curiously GFP, the most widely used labeling tag in cell biology, is rarely used for biochemical analyses, although various mono- and polyclonal antibodies have been described (9, 10). This may be due in part to limited availability and specificity as well as co-eluted heavy and light antibody chains that interfere with subsequent analyses. An alternative to conventional antibodies are variable single domain antibody fragments, also referred to as V_HH, derived from heavy chain antibodies of Camelidae (11). These V_HHs, which present the smallest intact antigen-binding units with a molecular mass of about ~15 kDa are highly soluble and stable and can be efficiently produced in heterologous systems (12, 13). V_HH fragments have been used like conventional antibodies for various immunological applications (14–16).

Here we describe a novel application of a 13-kDa GFP binding fragment derived from a llama single chain antibody (17). This GFP-binding protein (GBP) has a small (2.5 × 4.5-nm) barrel-shaped structure and can easily be produced in bacteria. We immobilized the GBP to generate a GFP-nanotrap, which enables a fast and efficient isolation of GFP fusion proteins and their interacting factors for biochemical and ChIP analyses. Moreover we demonstrated that the GFP-binding protein can be fused with structural proteins to ectopically recruit GFP fusion proteins and interacting factors at defined regions in living cells.

From the ‡Munich Center for Integrated Protein Science, (CiPS^M) and Department of Biology, Ludwig Maximilians University Munich, 82152 Planegg-Martinsried, Germany, §Department of Molecular and Cellular Interactions, VIB and Laboratory of Cellular and Molecular Immunology, Vrije Universiteit Brussel, 1050 Brussels, Belgium, ¶Departments of Gene Vectors, GSF-National Research Center for Environment and Health, 81377 Munich, Germany, and ‖Max Delbrueck Center for Molecular Medicine, 13125 Berlin, Germany

Received, July 26, 2007, and in revised form, October 15, 2007

Published, MCP Papers in Press, October 21, 2007, DOI 10.1074/mcp.M700342-MCP200

[1] The abbreviations used are: GFP, green fluorescent protein; GBP, GFP-binding protein; ChIP, chromatin immunoprecipitation; V_HH, variable domain of heavy chain antibody; HEK, human embryonic kidney; IgG, immunoglobulin G; YFP, enhanced yellow fluorescent protein; CFP, enhanced cyan fluorescent protein; DsRed, *Discosoma* genus red fluorescent protein; mRFP, monomeric red fluorescent protein; PCNA, proliferating cell nuclear antigen; H2B, histone H2B; Dnmt1, DNA methyltransferase I; PBD, PCNA binding domain; HMGA1a, high mobility group protein A1a; Igf, insulin-like growth factor; PML, promyelocytic leukemia protein.

EXPERIMENTAL PROCEDURES

Expression and Purification of the GBP—Llama immunization, V_HH library construction, and selection of the GBP were described previously (17). The coding sequence of the GFP-binding V_HH domain was cloned into the pHEN6 (18) vector using the NcoI and NotI restriction sites adding a C-terminal histidine (His_6) tag, and chemically competent *Escherichia coli* BL21 cells were transformed. For expression and purification a 500-ml *E. coli* culture was induced with 1 mM isopropyl β-D-1-thiogalactopyranoside for 20 h at room temperature. Bacterial cells were harvested by centrifugation (10 min at 5000 × *g*), and the pellet was resuspended in 10 ml of binding buffer (1× PBS, pH 8.0, 0.5 M NaCl, 20 mM imidazole, 1 mM PMSF, 10 μg/μl lysozyme). The cell suspension was incubated for 1 h at 4 °C in a rotary shaker and then sonified (6 × 10-s pulse) on ice. After centrifugation (20 min at 20,000 × *g*) soluble proteins were loaded on a preequilibrated 1-ml HiTrap column (GE Healthcare) and purified. The His-tagged GBP was eluted by a linear gradient ranging from 20 to 500 mM imidazole. Elution fractions containing the GBP were pooled and dialyzed into PBS. Protein concentration was adjusted to 1 μg/μl. The yield of purified GBP/liter of bacterial culture was in the range of 10–15 mg.

Expression Plasmids—For bacterial expression and purification of GFP we used the bacterial expression plasmid pRSet5D containing the GFP coding sequence with a C-terminal His_6 tag kindly provided by B. Steipe. For mammalian cells we used the following expression vectors encoding different fluorescent fusion proteins: pEGFP-C1, pEYFP-C1, pECFP-C1, GFP-β-actin (all from Clontech), GFP-Lamin B1 (19), GFP-PCNA (20), mRFP-PCNA, GFP-Dnmt1, and GFP-Dnmt1(P1229W) (21). We also used mammalian expression vectors containing cDNAs coding for mRFP1 (22), mCherry, or mOrange (23) kindly provided by R. Tsien. Overlap extension PCR was performed to construct the CFP I147N and the CFP T154M using mutagenic primers CFP-I147N-FW (5′-GAGTACAACTACAACAGCCACAACGTCTATA-3′) in combination with CFP-I147N-Rev (5′-AACGTCTATATCATGGCCGACAAGCAG-3′) and CFP-T154M-FW (5′-AACGTCTATATCATGGCCGACAAGCAG-3′) in combination with CFP-T154M-Rev (5′-CTGCTTGTCGGCCATGATATAGACGTT-3′), respectively, and the flanking primer CFP FW (5′-GATCCGCTAGCGCTACCGGTCGCCACCATG-3′) and CFP-Rev (5′-AACGTCTATATCATGGCCGACAAGCAG-3′). The PCR fragment was cloned into the NheI/BsrGI site of the pECFP-C1 vector. For GBP-Lamin B1, the Lamin B1 was amplified from GFP-Lamin B1 by PCR with primers LaminB1EcoRV#F (5′-CCCCGATATCGGCGACTGCGACCCCC-3′) and LaminB1HisNotI#R (5′-GGGGGCGGCCGCCTAGTGATGGTGATGGTGGTGTTACATAATTGCACAGCTTC-3′). The PCR product was purified, digested with EcoRV and NotI, and ligated into the EcoRV/NotI sites of the GFP chromobody vector. All resulting constructs were sequenced and tested for expression in HEK 293T cells followed by Western blot analysis.

Antibodies—For immunoprecipitation and immunoblotting a mixture of two anti-GFP monoclonal antibodies (clones 7.1 and 13.1) from Roche Diagnostics and an affinity-purified polyclonal anti-GFP antibody raised in rabbit (a kind gift from D. Nowak, Berlin, Germany) were used. Precipitated proteins were detected with antibodies against GFP, mRFP, Lamin B (H-90, Santa Cruz Biotechnologies), β-actin (monoclonal anti-β-actin, Sigma), and PCNA (monoclonal anti-PCNA, clone 16D10). Promyelocytic leukemia protein (PML) bodies were detected with a monoclonal anti-PML antibody (5E10).

Immunoprecipitation—1×10^6–1×10^7 HeLa, HeLa H2B-GFP, or HEK 293T cells either mock-treated or transiently transfected with expression vectors coding for GFP, YFP, CFP, mRFP, mCherry, mOrange, GFP-β-actin, GFP-Lamin B1, GFP-PCNA, or GFP-Dnmt1 were homogenized in 200 μl of lysis buffer (20 mM Tris/HCl, pH 7.5, 150 mM NaCl, 0.5 mM EDTA, 2 mM PMSF, 0.5% Nonidet P-40). For extraction of GFP-Lamin B1 or H2B-GFP the lysis buffer was modified by adding 0.5 M NaCl, 1 μg of DNase I, 5 mM $MgCl_2$, and 0.1% SDS. After a centrifugation step (10 min at 20,000 × *g* at 4 °C) the supernatant was adjusted with dilution buffer (20 mM Tris/HCl, pH 7.5, 150 mM NaCl, 0.5 mM EDTA, 2 mM PMSF) to 1 ml. 20 μl (2%) were added to SDS-containing sample buffer (referred to as input). 1 μg of purified GBP or 2 μg of anti-GFP antibodies were added and incubated for 5–60 min on an end-over-end rotor at 4 °C. For pulldown of immunocomplexes 25 μl of an equilibrated mixture of protein A/G-Sepharose (Amersham Biosciences) were added, and incubation continued for 60 min. After a centrifugation step (2 min at 5000 × *g* at 4 °C) supernatant was removed, and 2% was used for SDS-PAGE (referred to as flow-through). The bead pellet was washed two times in 1 ml of dilution buffer containing 300 mM NaCl. After the last washing step the beads were resuspended in 2× SDS-containing sample buffer and boiled for 10 min at 95 °C.

Column-based GFP Purification—1 mg of purified GBP was covalently coupled to 1 ml of *N*-hydroxysuccinimide-Sepharose (GE Healthcare), according to the manufacturer's instructions, generating the GFP-nanotrap. Subsequently 50 μl of the GFP-nanotrap was transferred to a 1-ml column (MoBiTec) and preequilibrated with 5 ml of dilution buffer. Protein extracts of GFP-producing cells were prepared as described above, and the soluble protein fraction was loaded onto the column. The protein solution (1 ml) passed through the column at 100–200 μl/min flow rate. Subsequently the column material was washed (two times) with 1 ml of dilution buffer containing 300 mM NaCl, and bound proteins were eluted with 100 μl 0.1 M glycine, pH 3.2. 2% of the input and flow-through and 10% of bound material were resuspended in 2× SDS-containing sample buffer and analyzed by SDS-PAGE and Coomassie Blue and by immunostaining.

Enzymatic Activity Test—Soluble protein extracts of HEK 293T cells producing GFP-Dnmt1 or GFP-Dnmt1(P1229W) were prepared, and immunoprecipitation was performed as described above. Beads containing the GBP-GFP-Dnmt1 complexes were washed extensively in dilution buffer containing 300 mM NaCl, and after centrifugation the beads were resuspended in 500 μl of assay buffer (100 mM KCl, 10 mM Tris, pH 7.6, 1 mM EDTA, 1 mM DTT). Beads were washed (two times) in assay buffer, and after centrifugation (1000 × *g* for 1 min) 30 μl of methylation mixture (0.1 μCi of *S*-[^{3}H]adenosylmethionine (Amersham Biosciences), 1.67 pmol/μl hemimethylated double-stranded 35-bp DNA (50 pmol/μl), 160 ng/μl BSA) were added. As a positive control 2 μg of recombinant purified DNA methyltransferase I (DNMT1) was used. Incubation was carried out for 2.5 h at 37 °C, and the reactions were spotted onto DE81 cellulose filters. Subsequently filters were washed (three times) with 0.2 M $(NH_4)HCO_3$, once with H_2O, and once with 100% EtOH. After drying at 80 °C the filter was transferred into a Mini-Poly-Q vial with 5 ml of Ultima Gold LSC Mixture (PerkinElmer Life Sciences), and each sample was measured for 1 min in a scintillation counter (Beckman LS1801). A sample without enzyme addition was used as negative control.

Chromatin Immunoprecipitation Assay and Real Time PCR Analysis—For chromatin immunoprecipitation experiments, formaldehyde was diluted to 1% in serum-free medium, and 15 ml were added to monolayers of C2C12 and C2C12/HMGA1a-GFP cells for 10 min at room temperature. The cross-link was stopped by adding 1.5 ml of 1.25 M glycine. After removal of the medium, cells were washed (two times) on plates with cold 1× PBS, scraped off, and washed again in cold 1× PBS and once with hypotonic LSB buffer (10 mM Hepes, pH 7.9, 10 mM KCl, 1.5 mM $MgCl_2$). Cells were resuspended in 2.7 ml of LSB buffer and lysed by adding 300 μl of 20% Sarkosyl. The chromatin was carefully layered onto a 40-ml sucrose cushion (LSB buffer plus 100 mM sucrose) and centrifuged (10 min at 4 °C at 4000 × *g*). Supernatant was removed, and the chromatin was resuspended in 2 ml of TE (10 mM Tris, 0.5 mM EDTA, pH 8.0) and sonicated (Branson sonifier 250-D, 35% amplitude, 2 min in 1-s intervals). For each

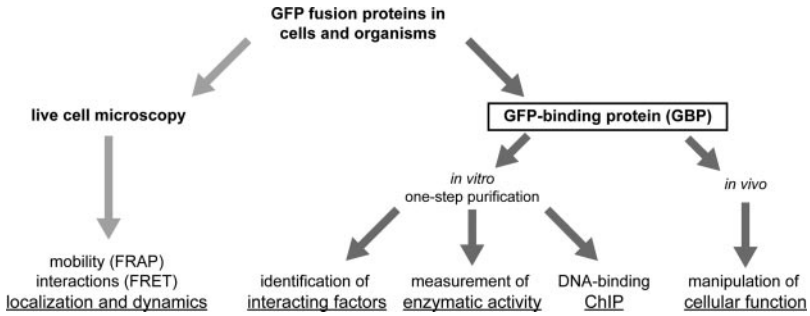

FIG. 1. **Outline of possible GFP fusion protein applications with the GFP-nanotrap.** *FRAP*, fluorescence recovery after photobleaching; *FRET*, fluorescence resonance energy transfer.

immunoprecipitation, 500 μg of the nucleoprotein were adjusted with 1/10 volume of 1× NET (50 mM Tris, 150 mM NaCl, 0.5 M EDTA, 0.5% Nonidet P-40). 10 μg of two anti-GFP monoclonal antibodies (clones 7.1 and 13.1; Roche Diagnostics), a mouse IgG1 isotype control, and 5 μg of GFP-nanotrap were incubated overnight at 4 °C. The purification of co-precipitated DNA was performed as described above. Real time PCR was performed with the Light Cycler instrument (Roche Diagnostics) using a ready-to-use "hot start" reaction mixture (FastStart DNA Master SYBR Green I; Roche Diagnostics). Real time PCR analysis was performed according to the manufacturer's instructions using the same parameters as described previously (24). The list of primer pairs is given in supplemental Table 1.

RESULTS

Ideally the subcellular localization and binding dynamics of fluorescent fusion proteins should be complemented with biochemical data on interacting factors, enzymatic activity, and DNA binding properties (Fig. 1). To generate a nanotrap for fast and efficient purification of GFP fusion proteins we used a small recombinant 13-kDa GBP comprising the epitope recognition domain of a heavy chain antibody raised in an alpaca (*Lama pacos*) against GFP (17). The GBP was fused with a C-terminal histidine (His_6) tag, produced in *E. coli*, and purified by IMAC (supplemental Fig. S1A). Subsequent gel filtration analysis showed a single elution peak at about 13 kDa indicating that the GBP can easily be produced and purified as a stable monomer (supplemental Fig. S1B). For a first functional analysis we tested the binding capacity of the GBP to purified GFP. Equimolar amounts of both proteins were mixed and incubated for about 20 min. Subsequent gel filtration analysis showed that the GBP and its antigen rapidly assemble into a stable, stoichiometric complex with a corresponding native molecular mass of 41 kDa (supplemental Fig. S2). We then tested the ability of GBP to precipitate its antigen from cell extracts and directly compared its performance with mono- and polyclonal anti-GFP antibodies. GBP and anti-GFP antibodies were added to protein extracts of HEK 293T cells expressing GFP. Precipitated proteins were separated by SDS-PAGE and visualized by Coomassie Blue or immunoblot analysis (Fig. 2*A*). After precipitation with GBP only two protein bands (GFP at ~28 kDa and the GBP itself at ~13 kDa) were detectable, whereas additional bands corresponding to the light and heavy chains of the denatured IgGs as well as unspecifically precipitated proteins could be observed in immunoprecipitations with the mono- and polyclonal anti-GFP antibodies. The quantitative comparison of precipitated GFP in relation to antibody input showed that the GBP is clearly more efficient than established mono- and polyclonal antibodies (Fig. 2*A* and supplemental Fig. S3).

Conveniently GBP complexes can be immobilized and precipitated with protein A-agarose just like conventional antibodies (Fig. 2*A*, *left panel*). However, to prevent elution of the GBP itself and to avoid any interference with subsequent analyses we covalently coupled GBP to *N*-hydroxysuccinimide-Sepharose beads generating a stable GFP-binding matrix (GFP-nanotrap). This GFP-nanotrap allowed a very fast (5-min) column-based purification of GFP from total cell extracts yielding a single protein band without any visible unspecific protein contamination (Fig. 2*B*, *right panel*). Moreover the immunoblotting analysis revealed a quantitative precipitation of the antigen visible as depletion of GFP from the flow-through fraction.

To analyze the specificity of GBP we performed immunoprecipitation with a set of different fluorescent proteins. Besides GFP itself, GBP recognizes the yellow variant YFP but not CFP or any derivatives of DsRed like mRFP, mCherry, or mOrange (supplemental Fig. S4). To further characterize the binding properties of GBP we tested different salt, temperature, and pH conditions. First, we increased the NaCl molarity of the binding buffer from 0.15 to 2 M and found that GBP precipitates its antigen even under high salt conditions (supplemental Fig. S5*A*). Second, we tested different incubation temperatures and observed quantitative precipitation of GFP even at 65 °C (supplemental Fig. S5*B*) demonstrating the temperature-stable folding and binding of GBP. Third, we tested the elution of bound epitope at different pH conditions. GFP was stably bound in the range from pH 4 up to pH 11. Lowering the pH to 3.2 caused quantitative release of GFP providing a fast and efficient method to elute bound antigen complexes from the GFP-nanotrap (supplemental Fig. S5*C*).

To investigate whether GBP also precipitates GFP fusion proteins we chose four well characterized constructs from different subcellular compartments: GFP-β-actin (25), GFP-Lamin B1 (26), GFP-PCNA (20), and H2B-GFP (27). Cells transiently or stably expressing the fusion proteins were analyzed by confocal microscopy to determine the subcellular localization of the GFP fusion protein (Fig. 2*B*, *upper panel*). Subsequently cells were harvested, and GFP fusion proteins

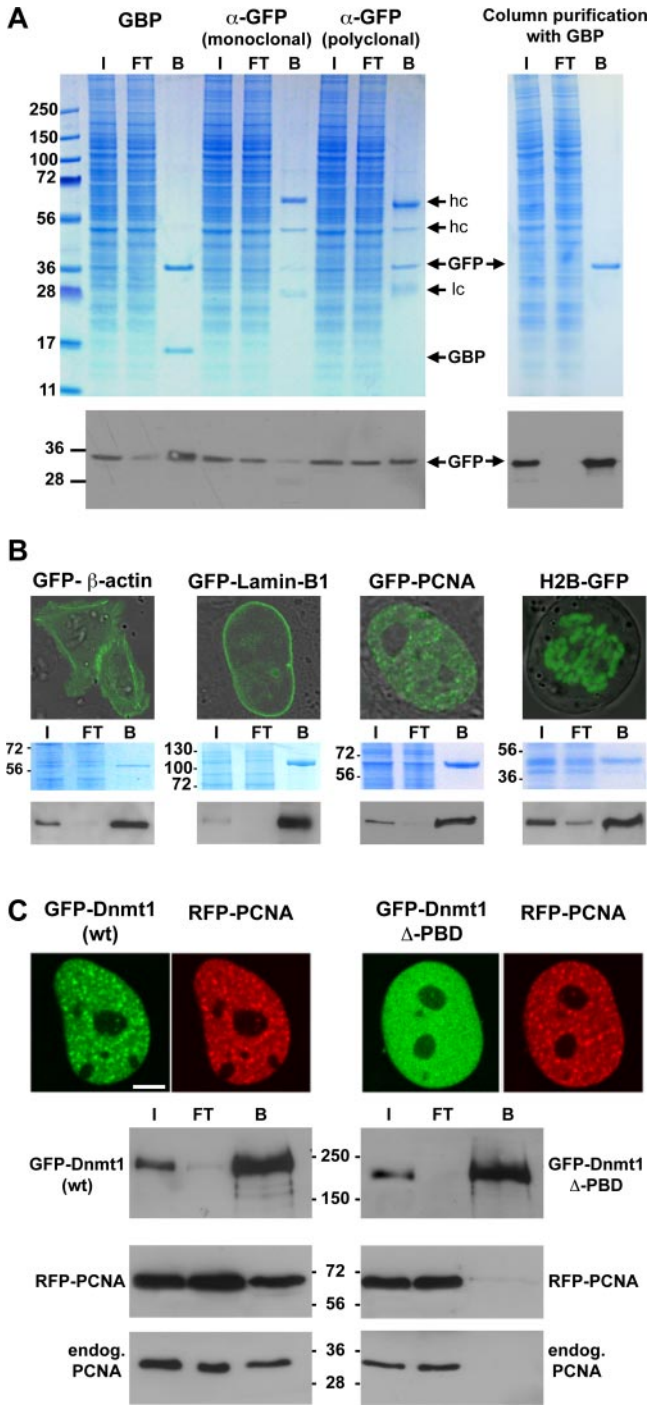

FIG. 2. **One-step purification of fluorescent proteins.** *A*, immunoprecipitation of GFP. *Left panel*, comparison of GBP with mono- and polyclonal anti-GFP antibodies. Protein extracts of GFP-producing HEK 293T cells were subjected to immunoprecipitation with GBP, mono-, or polyclonal anti-GFP antibodies. Throughout (*A–C*) aliquots of input (*I*), flow-through (*FT*), and bound fraction (*B*) were separated by SDS-PAGE and visualized either by Coomassie Blue (*top*) or by immunoblot analysis (*bottom*). Precipitated GFP, denatured heavy (*hc*) and light chains (*lc*) of the IgGs, and the GBP are marked by *arrows*. *Right panel*, column-based purification with the GFP-nanotrap. GFP-containing protein extracts were loaded on a column containing GBP directly coupled to Sepharose (GFP-nanotrap), and bound proteins were eluted. *B*, one-step purification of GFP fusion proteins with the GFP-nanotrap. Representative images of HeLa cells producing GFP-β-actin, GFP-Lamin B1, GFP-PCNA, or H2B-GFP are shown (*upper panel*). Cells were lysed, and GFP fusion proteins were one-step purified with the GFP-nanotrap. *C*, co-precipitation of GFP fusion proteins and interacting factors. HeLa cells coexpressing either GFP-Dnmt1 or a deletion mutant of Dnmt1 (GFP-Dnmt1Δ-PBD) together with the red fluorescent version of PCNA (mRFP-PCNA) were analyzed by live cell microscopy. Representative confocal images of two cells in early-to-mid S phase are shown (*scale bar*, 5 μm). Subsequently cells were lysed and subjected to immunoprecipitation with the GFP-nanotrap. *wt*, wild type.

were precipitated with the GFP-nanotrap followed by Coomassie staining and Western blot analysis (Fig. 2*B*, *lower panel*). The results show that GBP efficiently precipitated N- or C-terminal GFP fusion proteins from different subcellular compartments and structures.

One of the most interesting applications of the GBP is the possibility to correlate subcellular localization, dynamics, and complex formation of specific proteins and mutants thereof. We had previously identified a deletion mutant of Dnmt1 lacking the PCNA interaction domain (Dnmt1Δ-PBD) (28). In comparison with wild-type Dnmt1 (GFP-Dnmt1) the fluorescent labeled mutant (GFP-Dnmt1Δ-PBD) showed no colocalization with the red fluorescent PCNA (mRFP-PCNA) during S phase (Fig. 2*C*, *upper panel*). We then compared this observation from living cells with biochemical data. Cells were lysed immediately after microscopic analysis and subjected to immunoprecipitation with the GFP-nanotrap. Immunoblot analysis showed that mRFP-PCNA co-precipitates with GFP-Dnmt1 but not with GFP-Dnmt1Δ-PBD (Fig. 2*C*, *lower panel*). The unbound mRFP-PCNA fraction reflects the transient nature of the Dnmt1-PCNA interaction during S phase (21). In addition, we also detected endogenous PCNA co-precipitating with GFP-Dnmt1 but not with GFP-Dnmt1Δ-PBD, demonstrating that GBP can also pick up interacting endogenous proteins. These results show that the GFP-nanotrap is suitable to identify (even) transiently interacting factors and cell cycle-dependent complexes. Taking advantage of its avid and specific binding we now routinely use the GFP-nanotrap to identify interacting factors by MALDI mass spectrometry.

A critical question in live cell studies is whether the fluorescent fusion proteins are enzymatically active and have biochemical properties similar to their endogenous counterparts. For fast determination of enzymatic activity we chose fluorescent fusion constructs of the murine Dnmt1, which are actively investigated in our laboratory. With live cell microscopy we could not distinguish the active GFP-Dnmt1 (wild type) and an enzymatically inactive version, GFP-Dnmt1(P1229W) (Fig. 3, *upper panel*). After visualization of the fluorescent Dnmt1 constructs in nuclei of mammalian cells both proteins were one-step purified from cell extracts with the GFP-nanotrap (Fig. 3, *middle panel*) and directly assayed for enzymatic

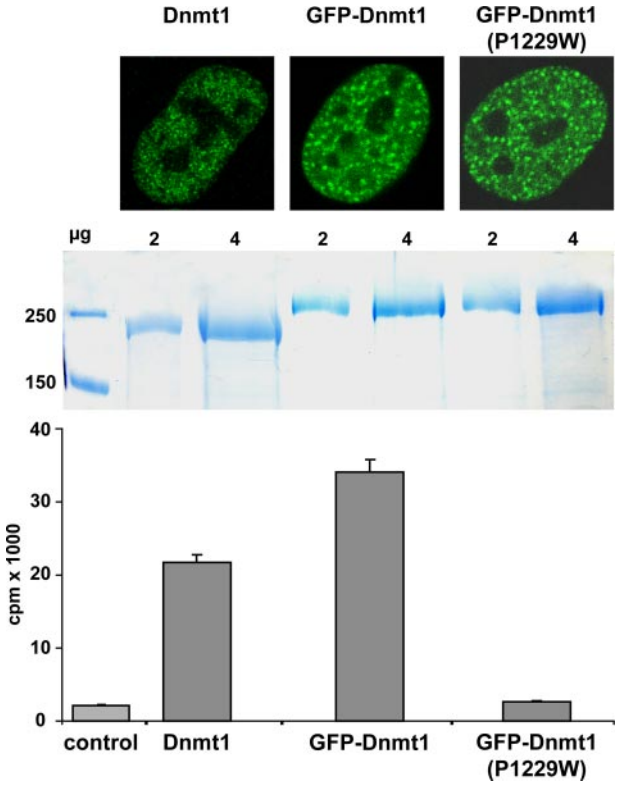

FIG. 3. **GFP fusion proteins retain their enzymatic activity after purification with the GFP-nanotrap.** Representative images of nuclei from HeLa cells show the endogenous Dnmt1, GFP-Dnmt1, or catalytically inactive mutant GFP-Dnmt1(P1229W) (*top*). Soluble protein extracts containing GFP-Dnmt1 or GFP-Dnmt1(P1229W) were one step-purified with the GFP-nanotrap and analyzed by SDS-PAGE followed by Coomassie Blue staining (*middle*). DNA methyltransferase activity of purified GFP fusion proteins (~4 µg each) and recombinant DNMT1 (~2 µg) were determined (*bottom*). $n = 4$; *error bars* show standard deviation.

measurements. GFP-Dnmt1 showed a specific DNA methyltransferase activity similar to that of purified recombinant DNMT1 (Fig. 3, *lower panel*). The comparison with the catalytically inactive GFP-Dnmt1(P1229W) revealed that the endogenous DNA methyltransferase activities of mammalian cells were efficiently removed by this quick one-step purification. These results demonstrate that the GFP-nanotrap is a highly efficient tool for quick and reliable biochemical characterization of fluorescent fusion proteins.

To investigate whether the GFP-nanotrap has the required specificity to function in chromatin immunoprecipitations we performed ChIP experiments using a mouse myoblast cell line stably expressing a GFP fusion of the high mobility group protein A1a (HMGA1a-GFP).[2] We analyzed the promoter regions of the Interleukin 6 and Igf-binding protein 1 genes that are known to preferentially bind HMGA1a (29–32). 500 µg of formaldehyde-cross-linked nucleoprotein were subjected to immunoprecipitation with the GFP-nanotrap and compared with commercially available GFP-specific antibodies. Only the GFP-nanotrap showed a reproducible 3-fold enrichment of promoter fragments over distal sites. This preferential binding of HMGA1a-GFP at the specific promoter sites was not detectable with conventional GFP-specific antibodies (Fig. 4). The parental C2C12 cells not expressing HMGA1a-GFP showed no specific enrichment of any sequences in comparison with the isotype control (data not shown). These data confirm the high specificity and sensitivity of the GFP-nanotrap.

These experiments show *in vitro* applications of the GFP-binding protein. In a second step we explored potential *in vivo* applications and placed the coding region of the GFP-binding protein at a defined position within the cell by fusing it to a structural component of the nuclear envelope. We fused the GBP with Lamin B1 (GBP-Lamin B1) to generate a cellular nanotrap at the nuclear lamina. As described above, GBP efficiently recognized and bound YFP but not the blue variant CFP *in vitro* (supplemental Fig. S4). To compare these biochemical data with binding specificity in living cells we transfected HeLa cells with GBP-Lamin B1, GFP, and CFP and determined the distribution of GFP and CFP with respect to the GFP-nanotrap positioned at the nuclear lamina. Confocal microscopy showed that only GFP was exclusively localized at the nuclear lamina, whereas CFP showed a strikingly different, disperse distribution throughout the cell (Fig. 5*A*). Sequence alignment of GFP, YFP, and CFP showed that CFP differs from the two other fluorescent proteins at two relevant amino acid positions (Fig. 5*B*). To define the epitope recognized by GBP we introduced single mutations reverting stepwise CFP to GFP. We found that the exchange of isoleucine at position 147 to asparagine (I147N) restored binding to the GFP-nanotrap, whereas mutating methionine at position 154 to a tryptophan (T154M) did not restore any detectable binding (Fig. 5*C*). This demonstrates the high selectivity and specificity of the GBP *in vitro* and *in vivo* even allowing detection of single amino acid substitutions. Finally we analyzed whether the GFP-nanotrap can be used to manipulate endogenous factors and cellular structures. As a target we chose the endogenous PML. The PML is organized in nuclear PML bodies, which play a role in regulation of gene expression, apoptosis, DNA repair, and proteolysis (33, 34). We could detect 10–30 PML bodies by immunofluorescence staining of PML in HeLa cells where PML bodies are evenly distributed throughout the nucleus (data not shown). In transiently transfected cells PML bodies are highlighted by the green fluorescence of the GFP-PML (35) fusion protein and immunostaining with a specific antibody against PML (Fig. 6*A*). Upon expression of GBP-Lamin B1 green fluorescent labeled PML bodies were exclusively found at the nuclear rim, and subsequent antibody staining confirmed the depletion of endogenous PML from the nuclear interior (Fig. 6*B*). These results demonstrate the potential of the GFP-nanotrap not only to recruit GFP fusion proteins but also interacting endogenous factors.

[2] J. Brocher and R. Hock, manuscript submitted.

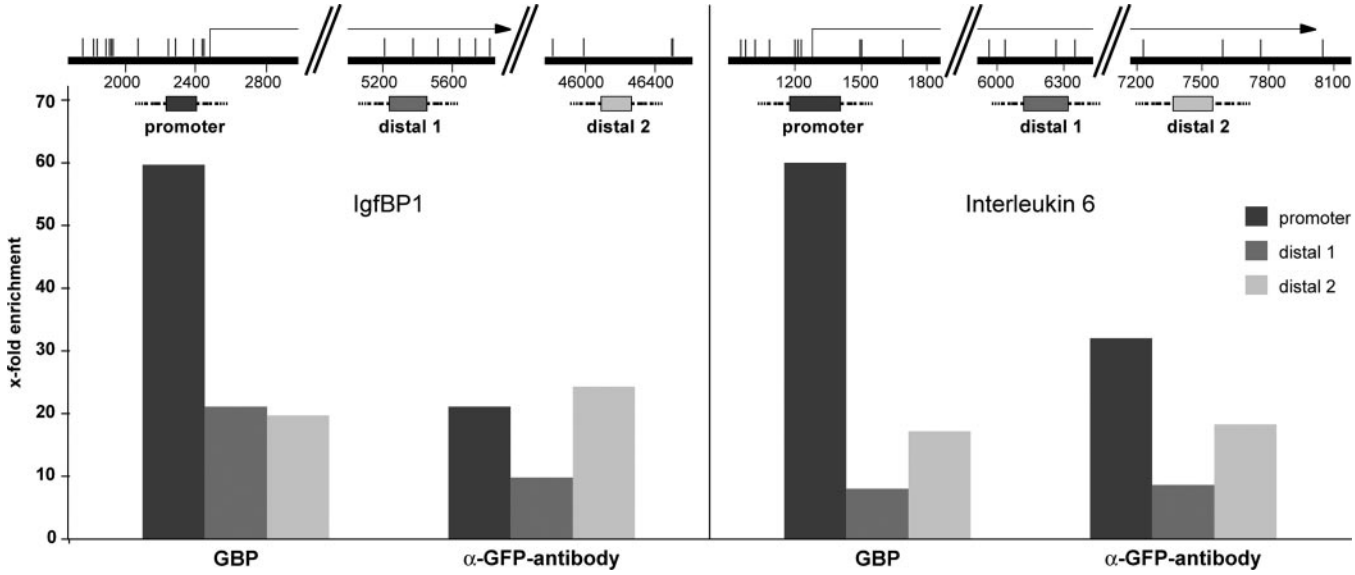

FIG. 4. **ChIP analysis with the GFP-nanotrap.** For ChIP experiments, 500 μg of C2C12/HMGA1a-GFP cells were subjected to immunoprecipitation using 5 μg of GFP-nanotrap, 10 μg of anti-GFP antibody (monoclonal), and 10 μg of mouse IgG1 isotype control, respectively. Co-precipitated DNA was quantified by real time PCR analysis using primer pairs of the IgfBP1 and Il6 promoter regions and indicated downstream regions (distal region 1/2). Results obtained for the Interleukin 6 and IgfBP1 promotor are shown in *dark gray*. *Column heights* indicate the relative enrichment obtained in two independent experiments as the difference between PCR values obtained with the GFP-nanotrap and anti-GFP antibodies over mouse IgG1 isotype control antibodies.

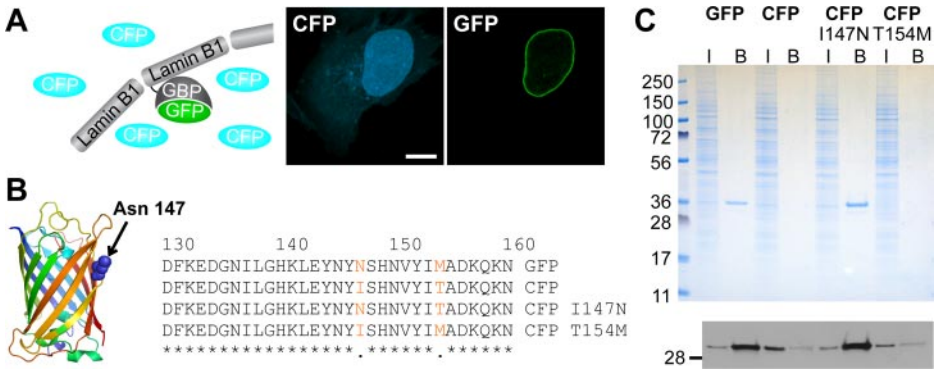

FIG. 5. **Specificity of the GFP-nanotrap.** *A*, in HeLa cells expressing GFP, CFP, and GBP-Lamin B1 GFP is exclusively localized at the nuclear lamina, whereas CFP is dispersedly distributed. *B*, amino acid sequence alignment of GFP, CFP, CFP I147N, and CFP T154M. Non-conserved residues are marked in *red*. The crystal structure of GFP (36) is shown, and the asparagine at position 147 is displayed as a *blue sphere* using PyMOL Version 0.99 (DeLano Scientific LLC). *C*, soluble protein extracts of HEK 293T cells expressing GFP, CFP, CFP I147N, and CFP T154M were subjected to one-step purification with the GFP-nanotrap. Input (*I*) and bound fractions (*B*) were separated by SDS-PAGE and analyzed by Coomassie Blue staining and by immunoblotting with anti-GFP antibody.

DISCUSSION

One challenge of the postgenomics era is the effective integration of genetic, biochemical, and cell biological data. This integration has in part been impeded by the simple fact that different protein tags are used for different applications. Here we present a GBP as a simple, robust, and versatile tool for biochemical analyses of GFP fusion proteins and even functional studies *in vivo*. The small and stable GBP has several decisive advantages over the conventional, 10 times larger, mono- and polyclonal antibodies. First, the GBP can be produced in bacteria in unlimited quantities and with reproducible quality and can easily be coupled to beads or matrices. Second, the high affinity of single chain GBP allows short (5–30-min) incubations to isolate fluorescent fusion proteins and even transiently bound factors from different cellular compartments. Third, its small size of about 13 kDa minimizes unspecific binding and entirely avoids contamination by heavy and light chains of conventional antibodies (50 and 25 kDa) that normally interfere with subsequent analyses.

The specificity of the GFP-nanotrap was further underlined by ChIP experiments with stable cells expressing a HMGA1a-GFP fusion. Analyzing DNA binding at two gene loci with the

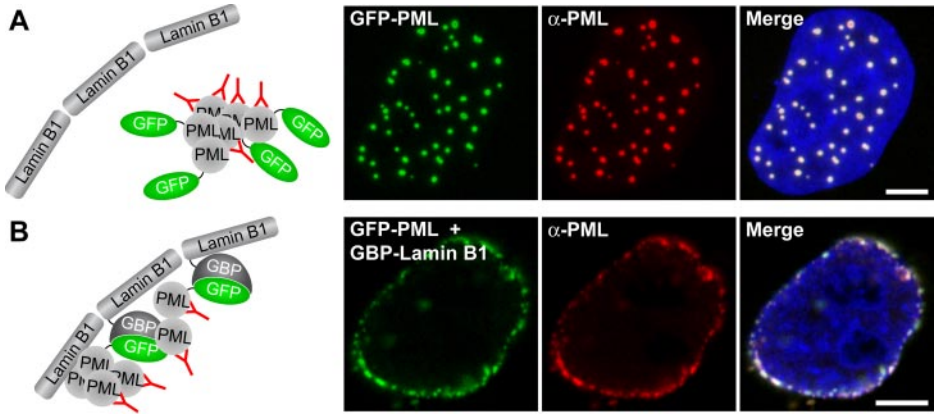

FIG. 6. **Targeted manipulation of nuclear structures with the GFP-nanotrap.** HeLa cells producing GFP-PML either alone or in combination with GBP-Lamin B1 are shown. Illustrating outlines are shown on the *left*. *A*, GFP-PML is assembled into endogenous PML bodies shown by immunofluorescence staining with an anti-PML antibody. *B*, coexpression of the GBP-Lamin B1 together with GFP-PML leads to a depletion of PML bodies from the nuclear interior shown by the absence of PML bodies in the nuclear interior after immunostaining with an anti-PML antibody.

GFP-nanotrap we detected a preferential binding of HMGA1a at the promoter regions that was far less evident with established anti-GFP antibodies.

In conclusion, this versatile GFP-nanotrap together with the widespread use of fluorescent fusion proteins now enables a fast and direct correlation of the subcellular localization and mobility of fluorescent fusion proteins with their enzymatic activity, interacting factors, and DNA binding properties combining cell biology and biochemistry with mutual benefits. Unlike conventional antibodies, the GFP-nanotrap can also be used for functional studies *in vivo*. We demonstrated that GBP can be fused with cellular proteins to set a GFP-nanotrap at a defined subcellular site to either ectopically recruit GFP fusion proteins and their associated factors or deplete them from their native surroundings. In one example we anchored the GBP at the nuclear lamina to capture nuclear bodies. Multiple other applications are possible because any GFP fusion protein can be combined with any cellular anchor point. The use of GBP as a nanotrap in living cells opens up an entire spectrum of new types of functional studies to probe and manipulate cellular processes and structures.

Acknowledgments—We thank A. Gahl and D. Nowak for excellent technical assistance; A. Jegg, J. Helma, R. Kleinhans, and K. Schmidthals for practical support; G. Längst and K. Dachauer for enzyme activity measurements; and R. Hock for the C2C12 HMGA1a-GFP cell line.

* This work was supported by the Center for NanoScience, by the Nanosystems Initiative Munich, and by grants from the Deutsche Forschungsgemeinschaft. The costs of publication of this article were defrayed in part by the payment of page charges. This article must therefore be hereby marked "*advertisement*" in accordance with 18 U.S.C. Section 1734 solely to indicate this fact.

S The on-line version of this article (available at http://www.mcponline.org) contains supplemental material.

** To whom correspondence should be addressed. E-mail: h.leonhardt@lmu.de.

REFERENCES

1. Chalfie, M., Tu, Y., Euskirchen, G., Ward, W. W., and Prasher, D. C. (1994) Green fluorescent protein as a marker for gene expression. *Science* **263,** 802–805
2. Misteli, T., and Spector, D. L. (1997) Applications of the green fluorescent protein in cell biology and biotechnology. *Nat. Biotechnol.* **15,** 961–964
3. Tsien, R. Y. (1998) The green fluorescent protein. *Annu. Rev. Biochem.* **67,** 509–544
4. van Roessel, P., and Brand, A. H. (2002) Imaging into the future: visualizing gene expression and protein interactions with fluorescent proteins. *Nat. Cell Biol.* **4,** E15–E20
5. Kellogg, D. R., and Moazed, D. (2002) Protein- and immunoaffinity purification of multiprotein complexes. *Methods Enzymol.* **351,** 172–183
6. Orlando, V., Strutt, H., and Paro, R. (1997) Analysis of chromatin structure by in vivo formaldehyde cross-linking. *Methods* **11,** 205–214
7. Fritze, C. E., and Anderson, T. R. (2000) Epitope tagging: general method for tracking recombinant proteins. *Methods Enzymol.* **327,** 3–16
8. Terpe, K. (2003) Overview of tag protein fusions: from molecular and biochemical fundamentals to commercial systems. *Appl. Microbiol. Biotechnol.* **60,** 523–533
9. Lorkovic, Z. J., Hilscher, J., and Barta, A. (2004) Use of fluorescent protein tags to study nuclear organization of the spliceosomal machinery in transiently transformed living plant cells. *Mol. Biol. Cell* **15,** 3233–3243
10. Cristea, I. M., Williams, R., Chait, B. T., and Rout, M. P. (2005) Fluorescent proteins as proteomic probes. *Mol. Cell. Proteomics* **4,** 1933–1941
11. Hamers-Casterman, C., Atarhouch, T., Muyldermans, S., Robinson, G., Hamers, C., Songa, E. B., Bendahman, N., and Hamers, R. (1993) Naturally occurring antibodies devoid of light chains. *Nature* **363,** 446–448
12. Sheriff, S., and Constantine, K. L. (1996) Redefining the minimal antigen-binding fragment. *Nat. Struct. Biol.* **3,** 733–736
13. Muyldermans, S. (2001) Single domain camel antibodies: current status. *J. Biotechnol.* **74,** 277–302
14. van Koningsbruggen, S., de Haard, H., de Kievit, P., Dirks, R. W., van Remoortere, A., Groot, A. J., van Engelen, B. G., den Dunnen, J. T., Verrips, C. T., Frants, R. R., and van der Maarel, S. M. (2003) Llama-derived phage display antibodies in the dissection of the human disease oculopharyngeal muscular dystrophy. *J. Immunol. Methods* **279,** 149–161
15. Jobling, S. A., Jarman, C., Teh, M. M., Holmberg, N., Blake, C., and Verhoeyen, M. E. (2003) Immunomodulation of enzyme function in plants by single-domain antibody fragments. *Nat. Biotechnol.* **21,** 77–80
16. Groot, A. J., Verheesen, P., Westerlaken, E. J., Gort, E. H., van der Groep, P., Bovenschen, N., van der Wall, E., van Diest, P. J., and Shvarts, A. (2006) Identification by phage display of single-domain antibody fragments specific for the ODD domain in hypoxia-inducible factor 1alpha. *Lab. Investig.* **86,** 345–356
17. Rothbauer, U., Zolghadr, K., Tillib, S., Nowak, D., Schermelleh, L., Gahl, A., Backmann, N., Conrath, K., Muyldermans, S., Cardoso, M. C., and Leonhardt, H. (2006) Targeting and tracing antigens in live cells with fluorescent nanobodies. *Nat. Methods* **3,** 887–889
18. Arbabi Ghahroudi, M., Desmyter, A., Wyns, L., Hamers, R., and Muyldermans, S. (1997) Selection and identification of single domain antibody fragments from camel heavy-chain antibodies. *FEBS Lett.* **414,** 521–526
19. Beaudouin, J., Gerlich, D., Daigle, N., Eils, R., and Ellenberg, J. (2002) Nuclear envelope breakdown proceeds by microtubule-induced tearing of the lamina. *Cell* **108,** 83–96
20. Leonhardt, H., Rahn, H. P., Weinzierl, P., Sporbert, A., Cremer, T., Zink, D., and Cardoso, M. C. (2000) Dynamics of DNA replication factories in living

cells. *J. Cell Biol.* **149,** 271–280
21. Schermelleh, L., Spada, F., Easwaran, H. P., Zolghadr, K., Margot, J. B., Cardoso, M. C., and Leonhardt, H. (2005) Trapped in action: direct visualization of DNA methyltransferase activity in living cells. *Nat. Methods* **2,** 751–756
22. Campbell, R. E., Tour, O., Palmer, A. E., Steinbach, P. A., Baird, G. S., Zacharias, D. A., and Tsien, R. Y. (2002) A monomeric red fluorescent protein. *Proc. Natl. Acad. Sci. U. S. A.* **99,** 7877–7882
23. Shaner, N. C., Campbell, R. E., Steinbach, P. A., Giepmans, B. N., Palmer, A. E., and Tsien, R. Y. (2004) Improved monomeric red, orange and yellow fluorescent proteins derived from Discosoma sp. red fluorescent protein. *Nat. Biotechnol.* **22,** 1567–1572
24. Schepers, A., Ritzi, M., Bousset, K., Kremmer, E., Yates, J. L., Harwood, J., Diffley, J. F., and Hammerschmidt, W. (2001) Human origin recognition complex binds to the region of the latent origin of DNA replication of Epstein-Barr virus. *EMBO J.* **20,** 4588–4602
25. Westphal, M., Jungbluth, A., Heidecker, M., Muhlbauer, B., Heizer, C., Schwartz, J. M., Marriott, G., and Gerisch, G. (1997) Microfilament dynamics during cell movement and chemotaxis monitored using a GFP-actin fusion protein. *Curr. Biol.* **7,** 176–183
26. Daigle, N., Beaudouin, J., Hartnell, L., Imreh, G., Hallberg, E., Lippincott-Schwartz, J., and Ellenberg, J. (2001) Nuclear pore complexes form immobile networks and have a very low turnover in live mammalian cells. *J. Cell Biol.* **154,** 71–84
27. Kanda, T., Sullivan, K. F., and Wahl, G. M. (1998) Histone-GFP fusion protein enables sensitive analysis of chromosome dynamics in living mammalian cells. *Curr. Biol.* **8,** 377–385
28. Easwaran, H. P., Schermelleh, L., Leonhardt, H., and Cardoso, M. C. (2004) Replication-independent chromatin loading of Dnmt1 during G2 and M phases. *EMBO Rep.* **5,** 1181–1186
29. Bustin, M., and Reeves, R. (1996) High-mobility-group chromosomal proteins: architectural components that facilitate chromatin function. *Prog. Nucleic Acids Res. Mol. Biol.* **54,** 35–100
30. Allander, S. V., Durham, S. K., Scheimann, A. O., Wasserman, R. M., Suwanichkul, A., and Powell, D. R. (1997) Hepatic nuclear factor 3 and high mobility group I/Y proteins bind the insulin response element of the insulin-like growth factor-binding protein-1 promoter. *Endocrinology* **138,** 4291–4300
31. Battista, S., Pentimalli, F., Baldassarre, G., Fedele, M., Fidanza, V., Croce, C. M., and Fusco, A. (2003) Loss of Hmga1 gene function affects embryonic stem cell lympho-hematopoietic differentiation. *FASEB J.* **17,** 1496–1498
32. Foti, D., Chiefari, E., Fedele, M., Iuliano, R., Brunetti, L., Paonessa, F., Manfioletti, G., Barbetti, F., Brunetti, A., Croce, C. M., and Fusco, A. (2005) Lack of the architectural factor HMGA1 causes insulin resistance and diabetes in humans and mice. *Nat. Med.* **11,** 765–773
33. Maul, G. G., Negorev, D., Bell, P., and Ishov, A. M. (2000) Review: properties and assembly mechanisms of ND10, PML bodies, or PODs. *J. Struct. Biol.* **129,** 278–287
34. Borden, K. L. (2002) Pondering the promyelocytic leukemia protein (PML) puzzle: possible functions for PML nuclear bodies. *Mol. Cell. Biol.* **22,** 5259–5269
35. Moller, A., Sirma, H., Hofmann, T. G., Rueffer, S., Klimczak, E., Droge, W., Will, H., and Schmitz, M. L. (2003) PML is required for homeodomain-interacting protein kinase 2 (HIPK2)-mediated p53 phosphorylation and cell cycle arrest but is dispensable for the formation of HIPK domains. *Cancer Res.* **63,** 4310–4314
36. Yang, F., Moss, L. G., and Phillips, G. N., Jr. (1996) The molecular structure of green fluorescent protein. *Nat. Biotechnol.* **14,** 1246–1251